ICAS 2021 SHANG HAI
International Council of the Aeronautical Sciences
32nd Congress of the International Council of the Aeronautical Sciences
September 6-10, 2021
Pudong Shangri-La, Shanghai, China

FAILURE PROCESS IDENTIFICATION IN C/SIC SAMPLES WITH A RANGE OF TENSILE PERFORMANCE USING ACOUSTIC EMISSION

Yongzhen Zhang[1,2], Xiaoyan Tong[1], Leijiang Yao[1], Andy T.Augousti[3]

[1] Laboratory of Science and Technology on UAV, Northwestern Polytechnical University, Xi'an 710065, China
[2] School of Aeronautics, Northwestern Polytechnical University, Xi'an 710072, China
[3] Faculty of Science, Engineering and Computing, Kingston University London, SW15 3DW UK

Abstract

C/SiC composites are important hot-structural materials for future aeronautical applications. However, due to the complexity of the processing method and microstructure, C/SiC often displays a varied mechanical performance. To identify the failure processes of C/SiC made of different size fiber bundles under mechanical load, acoustic emission (AE), an effective continuous damage monitoring technique, was used to monitor tensile tests of C/SiC composites. Combined with the SEM observation on the fracture surface, five damage mechanisms were identified, and their evolution was described. It was found: (1) the main damage mechanisms of C/SiC prepared by the precursor impregnation-pyrolysis (PIP) process under tensile load are matrix cracking, fiber cluster fracture, and fiber cluster pull-out friction; (2) the size of fiber bundles makes the distribution of matrix defects in fiber bundles vary greatly, which has an important influence on the macroscopic properties and damage evolution process of materials; (3) for the C/SiC composites with a lager fiber bundle, lots of matrix cracks appear in the matrix in the fiber bundle at the early stage of loading, which leads to the decrease of material stiffness, in the later stage of loading, the large energy damage such as fiber cluster fracture and matrix cracking between fiber bundles appear and increase rapidly, which accelerates the fracture failure process of the material.

Keywords: C/SiC, acoustic emission, damage mechanism, pattern recognition

1. Introduction

Carbon fiber toughened silicon carbide composite (C/SiC) has become one of the key materials for reusable thermal protection structures of aerospace vehicles and ultra-high sound speed aircraft due to its lightweight, high specific strength, high specific modulus, good thermal-mechanical properties, and impact resistance [1-3]. The precursor impregnation pyrolysis (PIP) process is generally used for the fabrication of C/SiC composites and has many advantages such as lower component fabrication time to reduce costs significantly and lower fabrication temperature [4]. However, due to the complexity of the processing method and microstructure, C/SiC often exhibits different mechanical performances. Therefore, the mechanical properties and damage evolution of C/SiC with different sizes of fiber bundles prepared by PIP under tensile load are of great importance and should be taken into account for the design of this kind of composites.

In recent years, researchers have conducted many investigations on the mechanical properties of C/SiC composites. They relied on physical information released from the internal changes in materials to describe the damage process, such as electrical resistance, acoustic emission (AE) [5-7]. AE is defined as the class of phenomena whereby transient elastic waves are generated by the rapid release of energy from a localized source or sources within a material [8]. AE, an effective continuous damage monitoring technique, provides the feasibility to continuously monitor the material under loading [9]. However, there are still some challenges in the application of AE in damage identification of ceramic matrix composites (CMCs), such as its complex propagation and attenuation processes within the material. Researchers have tried to solve this problem with unsupervised cluster analysis [10-11]. This method has been used to analyze several kinds of CMCs and identified that AE signals grouping has a strong correlation with damage mechanisms [5,10-13].

The aim of this research is to identify the damage mechanisms and evolution of C/SiC made of different sizes of fiber bundles by using an unsupervised pattern recognition method and AE data obtained from tensile tests. Principal component analysis (PCA) and a fuzzy C-means (FCM) algorithm are used to help realize AE data cluster analysis. Combining fracture surface observation, the damage mechanisms and their evolution of C/SiC with different sizes of fiber bundles were characterized.

2. Experimental

C/SiC was prepared by PIP process. The carbon fiber(T-300) bundles are provided by Toray Industries. The PCS/xylene solution prepared by polycarbosilane(PCS) and xylene was used as the impregnant. The pyrolysis is carried out at 1200 ℃, and the impregnation-pyrolysis process was repeated until the weight gain rate drops below 2%. The C/SiC was machined into straight strip samples, as shown in Figure 1.

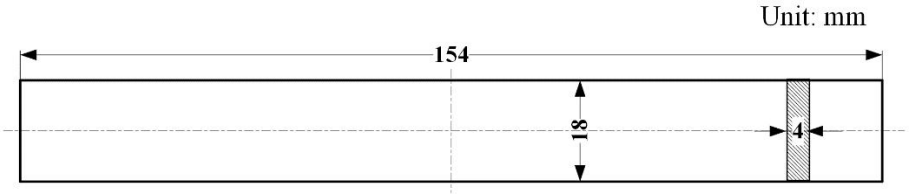

Figure 1 - Geometry of mechanical test specimens.

The room temperature mechanical tests were performed on a servo-hydraulic test machine (Model INSTRON 8801) with displacement-controlled loading. Two samples were tested and denoted by S1, S2. The bundle size of fiber in S1 is 1K, and that in S2 is 3K. Morphologies of the ruptured specimens were observed with a scanning electron microscope (TESCAN, VEGA 3 LMU).

The AE signals generated during the tests were detected by WD sensor (Physical Acoustic Corporation, PAC) attached to samples. AE data was collected during the tensile tests using the PCI-2 AE system (PAC), with a sampling rate 2MSPS. AE signals were frequency filtered between 20 kHz and 1MHz, pre-amplified by 40 dB. An amplitude threshold 40 dB was set to obtain AE hits. The installation of the sample and the AE sensor is shown in Figure 2. The diameter of the WD sensor is 16mm. A rubber band and a U-shaped metal sheet were used to fix the sensor at the center of the sample. Coupling agent is used between the sensor and the sample to eliminate the gap.

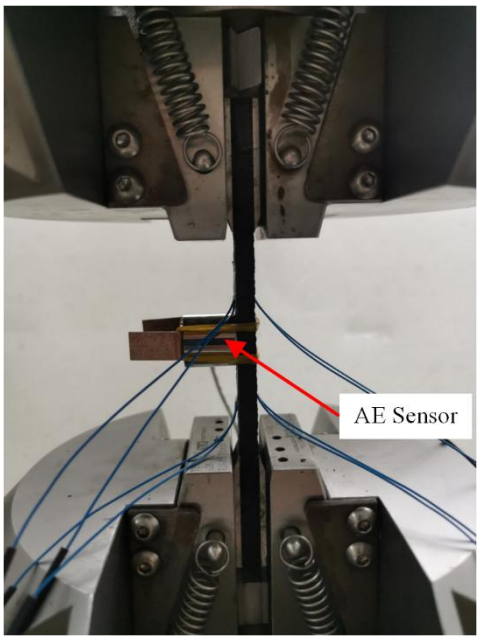

Figure 2 - Installation drawing of sample and AE sensor.

3. Pattern recognition techniques

The pattern recognition of AE signals is to establish the corresponding relationship between AE signals and damage mechanisms. The AE signals collected in mechanical tests are unlabeled data, so it is necessary to use an unsupervised clustering method to complete the pattern recognition. Figure 3 is the framework of AE pattern recognition. AE signals are generally described as rise time, counts, energy, amplitude, peak frequency, etc. AE signals are preprocessed and dimensionality reduced and clustered by FCM algorithm. Then, the AE signals and damage mechanism were matched by the analysis of material damage modes and fracture observation. Finally, the damage evolution of specimens is analyzed based on pattern recognition results.

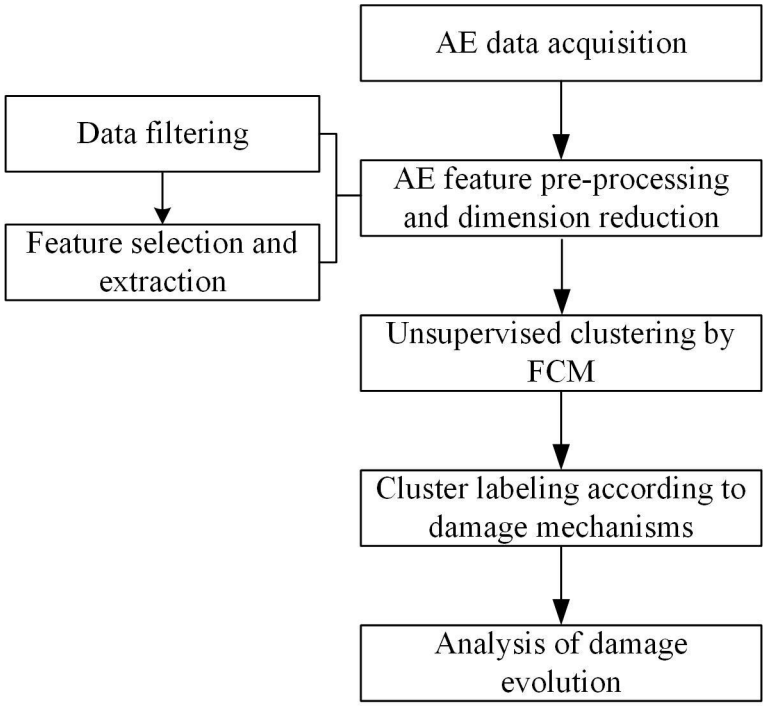

Figure 3 - The framework of AE pattern recognition.

3.1 Feature selection and extraction

In order to realize the reasonable classification of AE signals, the discrete characteristics of AE signals waveform are used as the basis of classification. However, redundant features may reduce the accuracy of classification and make the classification results unreliable. To avoid the problems, PCA, a most widely used data dimension reduction algorithm, is used to reduce dimension and extract features of AE signals. The main idea of PCA is to map n-dimensional features to k-dimensional features [14,15]. The k-dimensional features are new orthogonal features, also known as principal components, which are reconstructed from the original n-dimensional features. The selected principal components (PC) were the most representative eigenvectors, whose contributions were defined as corresponding collectively to more than 97 % of the data set standard deviation.

3.2 Unsupervised clustering algorithm and clustering validity

The fuzzy c-means (FCM) algorithm, developed by Dunn in 1973 [16] and improved by Bezdek in 1981 [17], is one of the most widely used fuzzy clustering algorithms. FCM is an algorithm that uses membership degree to determine whether each data point belongs to a certain clustering degree. The clustering algorithm is an improvement of traditional hard clustering algorithm. Compared with K-means algorithm, FCM provides more flexible clustering results to eliminate the influence of initial cluster centers.

Calinski-Harabasz index (CH) [18], Davies Bouldin (DB) [19]and Silhouette (Silh) index [20] were selected to check the validity of the clustering result. The larger CH index and Silh index, the smaller the DB index, the better the clustering result is.

4. Results and discussion

4.1 Tensile test and AE monitoring results

The mechanical tests are tensile tests of S1 and S2. The mechanical test and the AE monitoring results are given in Figure4. It is found that the tensile strength of C/SiC composites prepared by 1K fiber bundle is 211.8MPa, while that of C/SiC composites prepared by 3K fiber bundle is only 78.1MPa. At the same time, there are some differences in the AE process between the two samples. The high energy AE signals of S1 appeared in the middle stage of loading, while the high energy AE signals of S2 mainly concentrated in the later stage. In general, the AE energy of S2 is higher than that of S1.

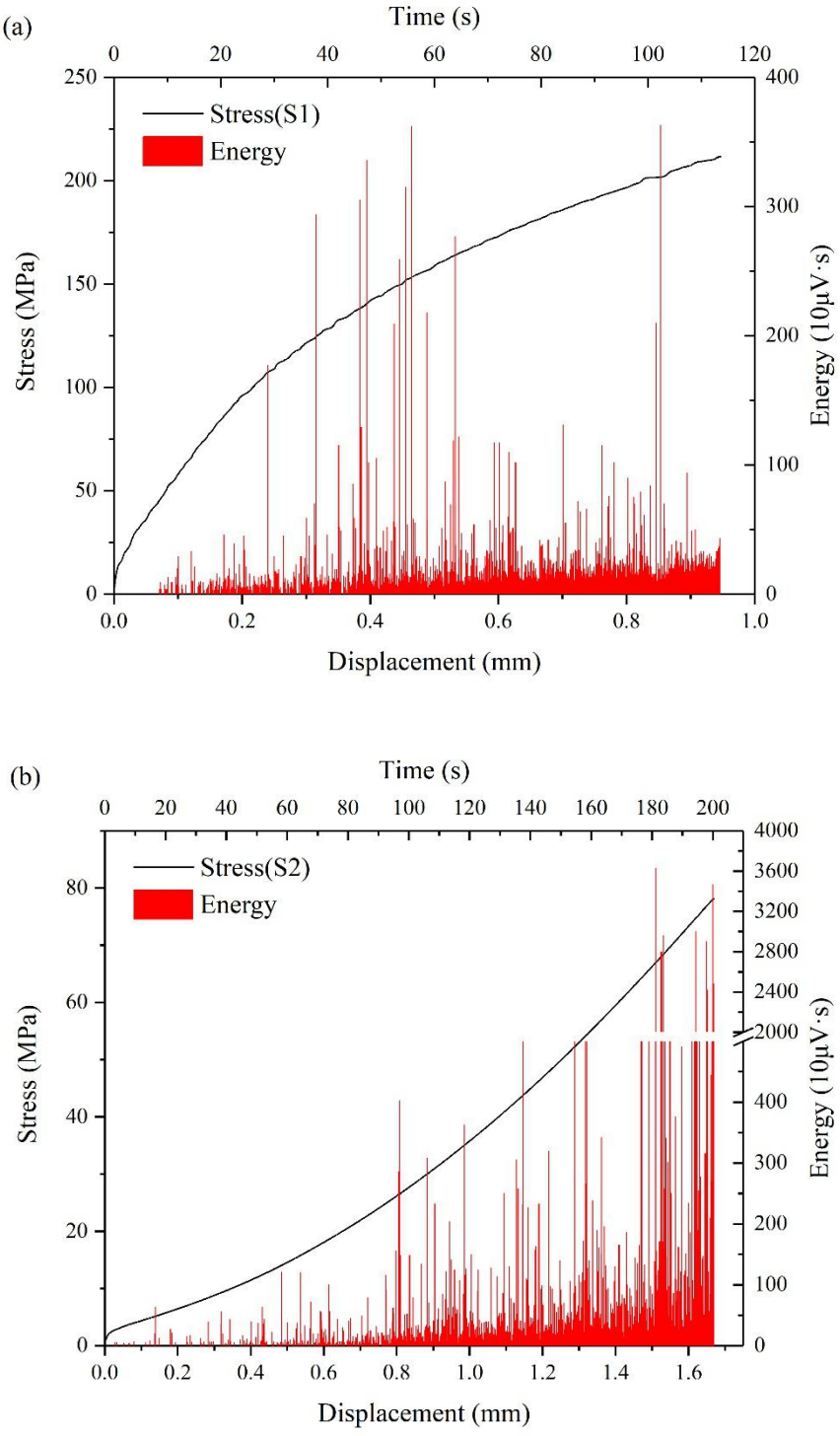

Figure 4 – The stress-displacement curve and AE energy during tensile tests.

4.2 Description of specimen fracture damage

The fracture surface of the specimens (Figure 5) reveals the material damage modes under tensile stress. Figure 5 (a), (b), (c) and (d) are SEM images of S1, and Figure 5 (e) (f) (g) and (h) are SEM images of S2. It can be found from the fracture surface that there are matrix cracks in fiber bundle, matrix cracks between fiber bundles and fiber cluster breakage. The fracture processes of single fiber and fiber clusters are accompanied by fiber pull-out friction and cluster pull-out friction. Comparing with Figure 5 (a) and Figure 5 (e), it is found that in S1, the fiber bundles are relatively close and the filled SiC matrix is less. While in S2, the distance between fiber bundles is larger and the matrix between fiber bundles is more, which can clearly distinguish the fiber and matrix. Comparing with Figure 5 (c) and Figure 5 (g), it is found that the fiber bundles of S1 fracture surface are relatively dispersed. But in S2, the fibers are more compact, which shows a large fiber cluster fracture composed of more fibers.

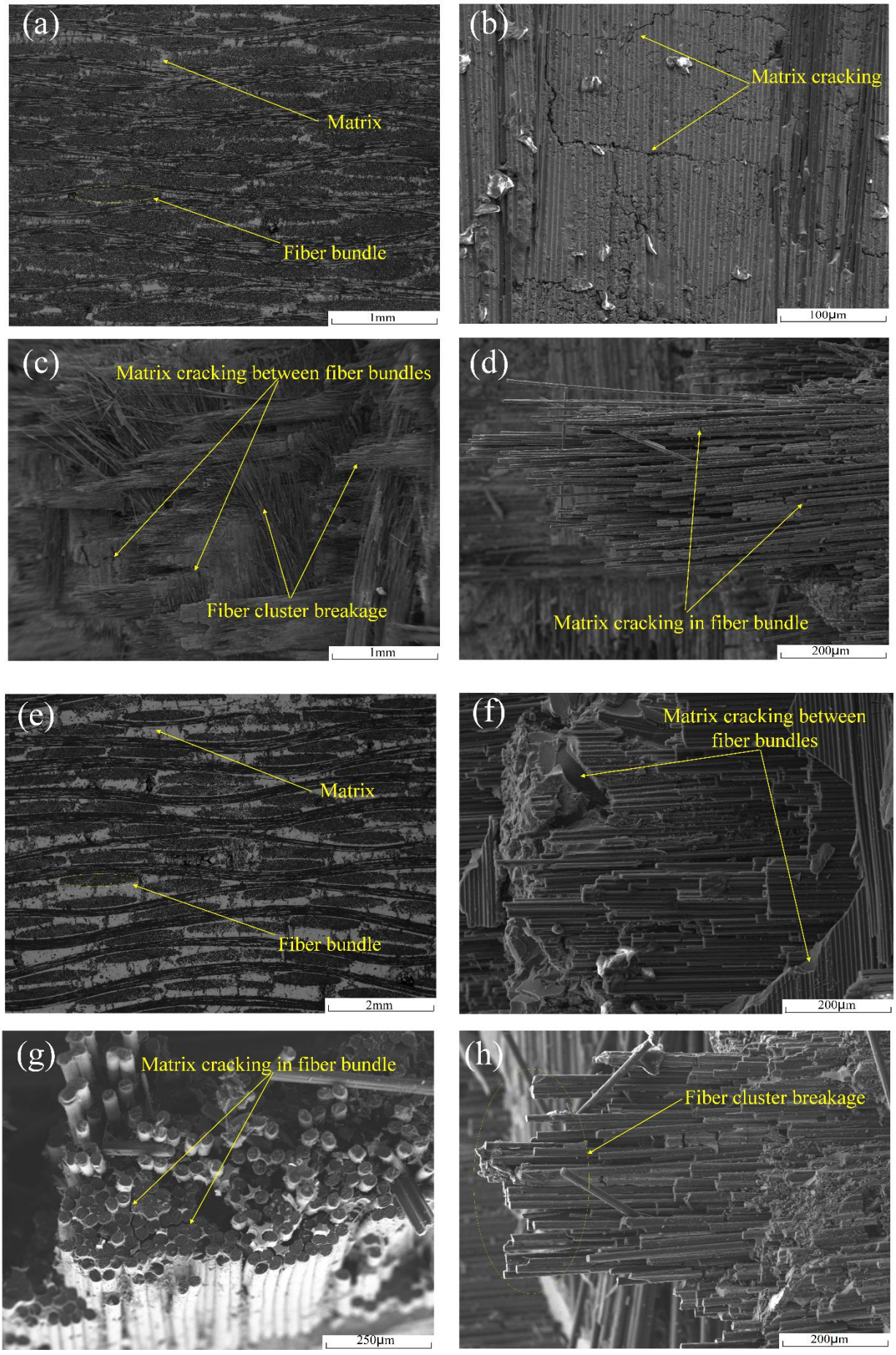

Figure 5 - The SEM micrographs of the fracture surfaces: (a), (b), (c) and (d) are the images of S1; (e), (f), (g) and (h) are the images of S2.

4.3 Pattern recognition results

Although the fiber bundle sizes of S1 and S2 are different, the preparation process and materials of the samples are identical. Therefore, it is believed that the microdamage forms of the two specimens are similar during loading. The difference in the final material properties between the two specimens depends on the evolution of damage mechanisms. In order to achieve the comparability of the results of unsupervised analysis of AE signals, the AE signals of S1 and S2 are fused to form an unsupervised clustering AE signals set that included six features: rise time, counts, energy, duration, amplitude, and peak frequency. PCA is performed on the AE data set, and four principal components are extracted. FCM clustering algorithm is used to cluster AE data. Figure 5 shows the CH index, DB index, and Silh index. The larger the value of CH index and Silh index, and the smaller the value of DB, the better the clustering result. It is found that the number of clusters c=5 gives the best result. Therefore, the AE events of the two samples can be divided into five classes. Table 1 summarizes the average characteristics of each AE signal cluster in S1 and S2.

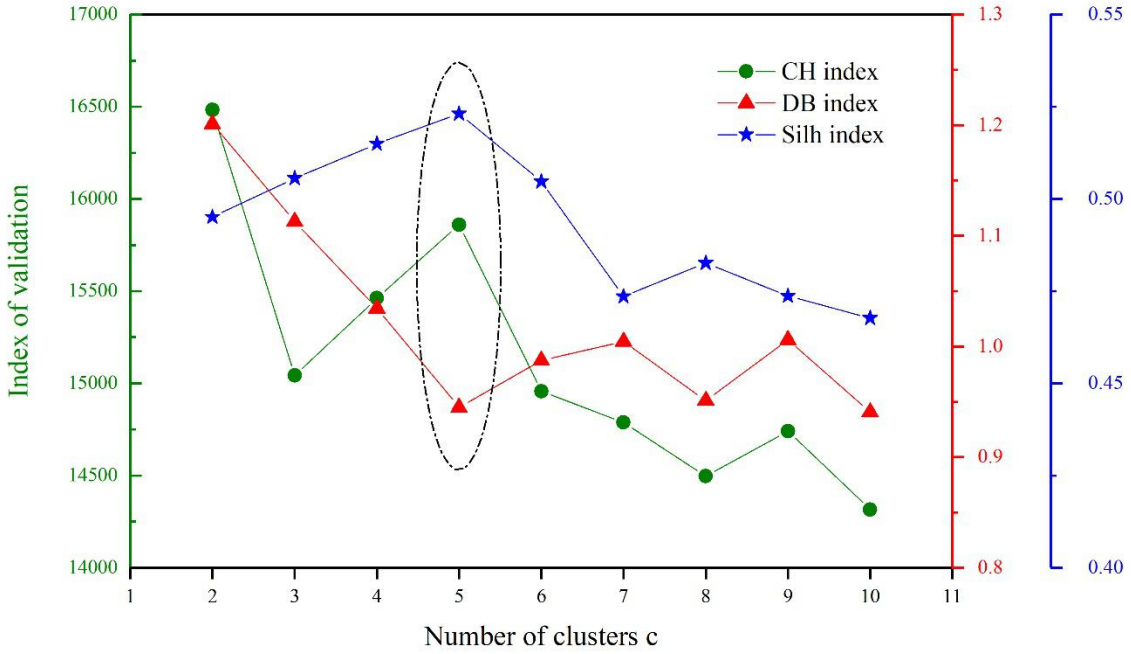

Figure 6 Index values obtained from different number of clusters.

In the process of loading, different damage can produce different AE signals. It is reasonable to believe that each class represents one kind of damage mechanism, and the center of each class reflects the basic physical foundation of corresponding damage mechanism. The AE energy is related to the energy released by the AE source and depends on the size of the source and the stored elastic energy [14]. Frequency depends to a large extent on the properties of compositions involved in the micro-fracture process [13]. Thus, cluster labelling can be proposed according to the peak frequency and AE energy.

The peak frequencies of class B and class D are higher than 400kHz, which belong to high frequency signals and are obviously different from other signals. At the same time, the matrix transfers the load to the fibers through the close contact with them. When the local load exceeds the fiber strength, the fibers begin to fracture. The broken fibers will be pulled out from the matrix with the loading. In Figure 5 (d) and (h), fiber clusters and fibers pullout after fracture can be observed. In the process of fibers and fiber clusters pulling out from the matrix, the friction between fiber and matrix is inevitable, and the corresponding AE signals are generated. At the same time, the friction is also a toughening mechanism of CMCs. Comparing the AE energy of Class B and Class D, it is found that the AE energy of Class D is higher than that of Class B, so Class D corresponds to the friction during the pulling out process of fiber cluster, and Class B corresponds to the friction during the pulling out process of single fiber or a few fibers. Therefore, Class B and Class D are named friction of fiber pullout and friction of fiber cluster pullout, respectively.

The peak frequencies of Class A and Class C are close to each other, which indicates that these

two kinds of signals may be the same kind of AE signals. However, the energy, counts, duration, and amplitude of Class A are larger than those of Class C, indicating that the damage area of Class A is larger than that of Class C. During the damage process of CMCs, the matrix inside and between fiber bundles will crack. The matrix in the fiber bundle is mostly small cracks due to the obstruction of the fiber. In the fiber bundles, there are large pores, and the matrix cracking is less hindered by the fiber. Large matrix cracks often appear. In Figure 5(c) (d) (e) and (h), two different types of matrix cracks can be found. Therefore, Class A corresponds to matrix cracking between fiber bundles, and Class C corresponds to matrix cracking in fiber bundle.

Finally, the unlabeled Class E corresponds to the fracture of fibers and fiber clusters. Fiber plays a toughening role in CMCs. After the material is loaded, the matrix around the fiber cracks, and the fiber bearing stress is higher. Therefore, the AE energy generated by the fibers and fiber clusters is larger. It can be seen from the classes' parameters of S1 and S2 that the AE energy of Class E is the largest. The AE energy of Class E in S2 is much larger than that in S1, which indicates that the broken fiber clusters in S2 is larger than that in S1. This phenomenon can be confirmed in Figure 5 (c) and (g).

Table 1 - AE features of the cluster centers

Sample. No	Risetime (ms)	Count	Energy (10μV·s)	Duration (μs)	Amplitude (mV)	Peak-Frequency (kHz)	Class
All specimens	186	47	20	755	60	66	A
	82	40	7	323	61	443	B
	100	28	7	348	58	58	C
	260	53	16	759	61	472	D
	586	54	20	848	59	144	E
S1	195	41	11	758	58	65	A
	128	28	5	365	58	476	B
	123	22	5	371	56	61	C
	272	45	9	765	59	479	D
	590	52	13	851	59	144	E
S2	108	88	93	731	72	79	A
	53	47	9	296	63	422	B
	52	40	10	302	63	51	C
	200	94	50	728	70	436	D
	520	82	147	798	68	151	E

4.4 Damage evolution analysis based on AE pattern recognition

When the AE signals in the loading process are classified and the corresponding damage mechanisms are identified , the damage evolution during the whole tensile process can be described. The cumulative number and cumulative AE energy of each class with displacement and time is shown in Figure 7 and Figure 8, respectively. For comparison purposes, cumulative number and cumulative energy are expressed as percentages.

For sample S1, from the perspective of AE energy, Class A, Class D and Class E are the main damage modes. Before the stress reaches 147.7MPa, at the initial stage of loading, the main damage is the matrix cracking in the fiber bundle represented by Class C. This kind of matrix crack belongs to small matrix crack and appears very early, and the AE energy is very small. It began to appear when the material was loaded, and developed gradually, converging into larger cracks. After the stress exceeded 147.7MPa, Class A, which represents the large matrix cracking between fiber bundles, became the main damage mode and developed rapidly with the increase of load. With the rapid development of matrix cracking between fiber bundles represented by Class A, the load of fiber bundles increased greatly. The number of the fiber cluster fracture and pull-out friction events also increased rapidly. When stress exceeded 185MPa, the matrix cracking between fiber bundles became the main damage mechanism.

For sample S2, it can be seen from Figure 7 (b) and Figure 8 (b) that before the stress reached 26.2MPa (Displacement:0-0.8mm) the AE signals were relatively fewer, and the AE energy was low. However, the number of Class C and Class B events representing matrix cracking in the fiber bundle and friction of fiber pull-out was more than that of other damage mechanisms, indicating that these two types of damage mainly develop in the early stage of loading. At the same time, when the stress reached 26.2MPa, the loading displacement were as high as 0.8mm. However, when the stress reached 147.7MPa, the loading displacement of S1 was only 0.43mm. The macro stiffness of the S2 with lager fiber bundle(3K) is obviously lower than that of the S1 with smaller fiber bundle(1K). Under the low stress level of 0~26.2MPa, in the fiber bundle, the matrix close to the defects and holes began to crack, forming a large number of microcracks. The generation and development of such microcracks may be one of the important reasons for the decrease of S2 stiffness. With the increase of loading, the AE energy of Class A and Class D increases rapidly. When the stress reached 66.3MPa, the large energy damage represented by Class A, Class D, and Class E occurred rapidly, and the material damage intensified until S2 fracture failure. From the time of appearance of damage, Class A, which represents matrix cracking between fiber bundles, began to appear at 51.7s. Class E, which represents the fiber cluster fracture, began to appear in 53.4s. In the later stage of loading, the damage of large fiber cluster made the local stress redistribute, increased the local stress in the undamaged area, and accelerated the overall failure of S2.

The above analysis found that: (1) whether in S1 or S2, matrix cracking between fiber bundles represented by Class A, fiber cluster pull-out friction represented by Class D, and fiber cluster fracture represented by Class E, are the main damage mechanisms. (2) In the aspect of cumulative energy and cumulative number of AE events, Class A, Class D, and Class E are consistent, while Class B and Class C are consistent. This conclusion reflects the synchronous occurrence of matrix cracking, fiber cluster fracture, and fiber cluster pull-out friction during the damage process of CMCs, which proves the correctness of the corresponding relationship between AE signals and damage mechanisms. (3) The damage development of S1 with a smaller fiber bundle is relatively stable in the whole process, while S2 with a larger fiber bundle is not obvious in the early stage of loading. However, in the later stage, the large cracking of the matrix between the fiber bundles and the large-area fracture of the fiber cluster, lead to the accelerated failure phenomenon, which eventually leads to the overall fracture of S2 at lower stress.

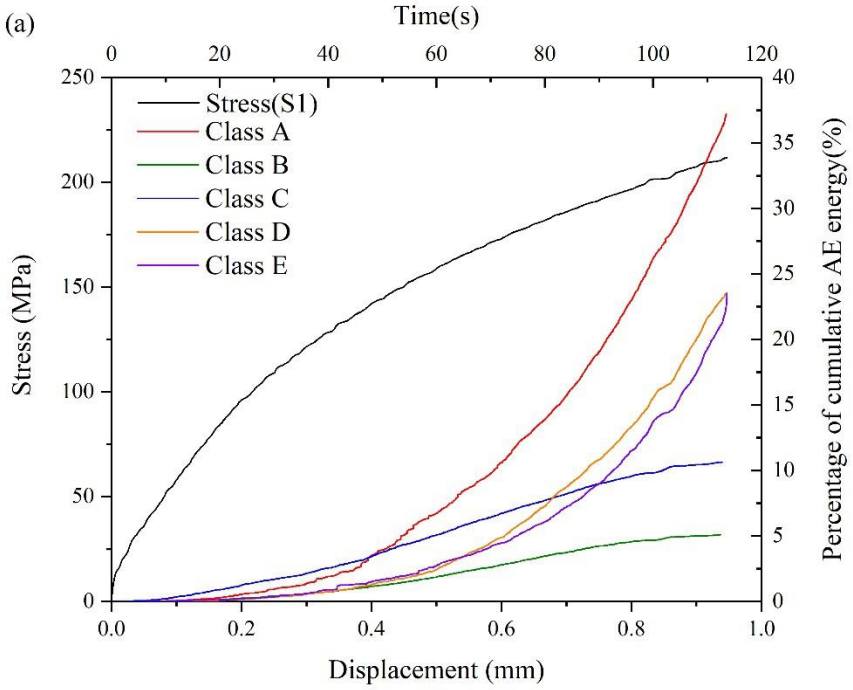

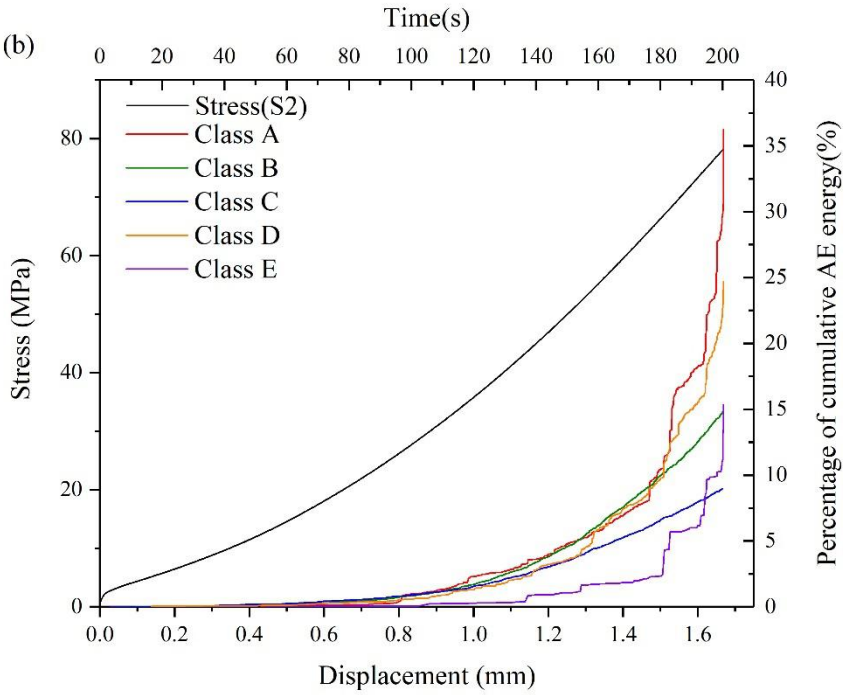

Figure 7 - The development of cumulative energy percentage with displacement and time: (a)S1; (b)S2

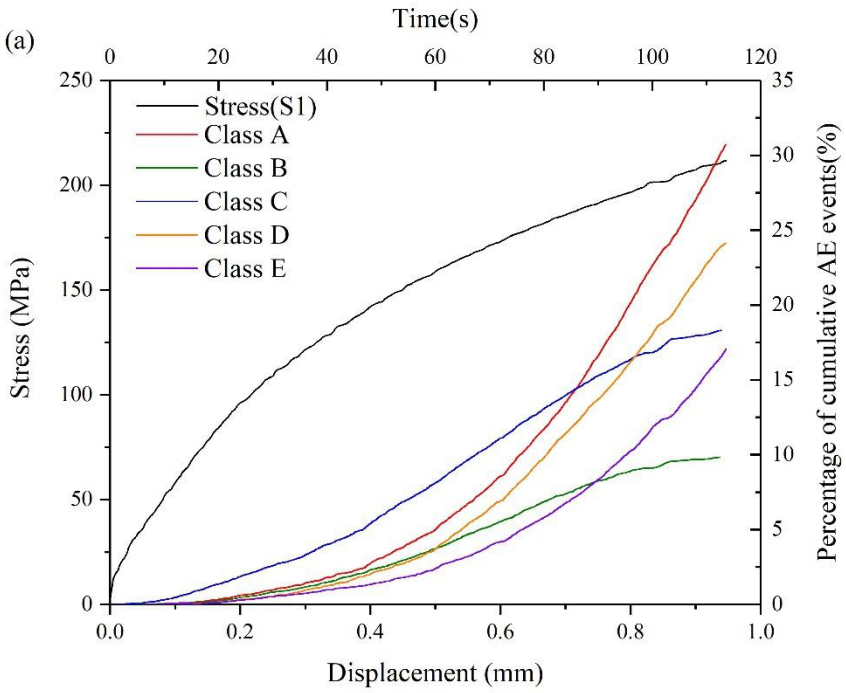

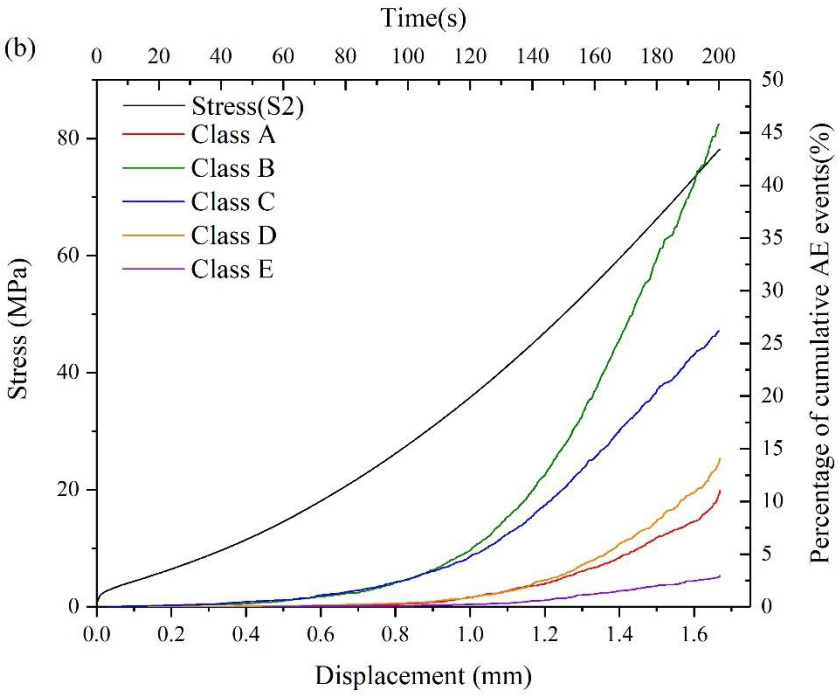

Figure 8 - The development of cumulative events percentage with displacement and time: (a)S1;(b) S2.

5. Conclusions

(1) The pattern recognition method based on AE can accurately identify the damage mechanisms and their evolution of C/SiC composites prepared by the PIP process under tensile load.

(2) The main damage modes of C/SiC prepared by the PIP process under tensile load are matrix cracking, fiber cluster fracture, and fiber cluster pull-out friction.

(3) The size of fiber bundles makes the distribution of matrix defects in fiber bundles vary greatly, which has an important influence on the macroscopic properties and damage evolution process of materials. For the C/SiC composites with large fiber bundles, in the early stage of loading, there are more cracks in the matrix in the fiber bundle caused by the material preparation defects, resulting in a decrease in material stiffness. In the later stage, the large energy damage such as fiber cluster fracture and matrix cracking between fiber bundles appear and increase rapidly; the local stress in the material redistributes and increases rapidly in the undamaged area, which leads to the damage acceleration and the ultimate strength of the material decreases.

6. Contact Author Email Address

Leijiang Yao: yaolj@nwpu.edu.cn

7. Copyright Statement

The authors confirm that they, and/or their company or organization, hold copyright on all of the original material included in this paper. The authors also confirm that they have obtained permission, from the copyright holder of any third party material included in this paper, to publish it as part of their paper. The authors confirm that they give permission, or have obtained permission from the copyright holder of this paper, for the publication and distribution of this paper as part of the ICAS proceedings or as individual off-prints from the proceedings.

References

[1] Naslain R. Design, preparation and properties of non-oxide CMCs for application in engines and nuclear reactors: an overview. *Composites Science & Technology, Vol.* 64, No. 2, pp 155-170, 2004.

[2] Krenkel W. Carbon Fiber Reinforced CMC for High−Performance Structures. *International Journal of Applied Ceramic Technology*, Vol. 1, No. 2, pp 188-200, 2005.

[3] Mei H, Cheng L, Ke Q, et al. High-temperature tensile properties and oxidation behavior of carbon fiber

reinforced silicon carbide bolts in a simulated re-entry environment. *Carbon*, Vol. 48, No. 11, pp 3007-3013, 2010.

[4] Li G, Zhang C, Hu H, et al. Preparation and mechanical properties of C/SiC nuts and bolts. *Materials Science & Engineering A*, Vol. 547, pp 1-5, 2012.

[5] Lyu P, Yao L, Ma X, et al. Correlation between failure mechanism and rupture lifetime of 2D-C/SiC under stress oxidation condition based on acoustic emission pattern recognition. *Journal of the European Ceramic Society,* Vol, 40, No. 15, pp 5094-5102, 2020.

[6] Smith CE, Morscher GN, Xia ZH. Monitoring damage accumulation in ceramic matrix composites using electrical resistivity. *Scripta Materialia*, Vol. 59, No. 4, pp 463-466, 2008.

[7] Yang X, Feng C, Peng Z-h, et al. Evolution of microstructure and mechanical properties of PIP-C/SiC composites after high-temperature oxidation. *Journal of Asian Ceramic Societies*, Vol. 5, No. 3, pp 370-376, 2017.

[8] Eitzen DG, Wadley HNG. Acoustic Emission: Establishing the Fundamentals. *Journal of Research of The National Bureau of Standards*, Vol.89, No. 1, pp 75-100,1984.

[9] T. Nozawa, K. Ozawa, Y. Asakura, A. Kohyama, H. Tanigawa, Evaluation of damage accumulation behavior and strength anisotropy of NITE SiC/SiC composites by acoustic emission, digital image correlation and electrical resistivity monitoring, *Journal of Nuclear Materials*, Vol. 455, No. 1-3, pp 549-553, 2014.

[10]Nair A, Cai CS, Kong X. Acoustic emission pattern recognition in CFRP retrofitted RC beams for failure mode identification. *Composites Part B-Engineering*, Vol.161, pp 691-701, 2019.

[11]Behnia A, Chai HK, GhasemiGol M, et al. Advanced damage detection technique by integration of unsupervised clustering into acoustic emission. *Engineering Fracture Mechanics*, Vol. 210, pp 212-227,2019.

[12]Yongzhen Z, Xiaoyan T, Leijiang Y, et al. Acoustic Emission Pattern Recognition on Tensile Damage Process of C/SiC Composites Using an Improved Genetic Algorithm. *Journal of Inorganic Materials*, Vol. 35, No. 5, pp 593-600,2020.

[13]Momon S, Godin N, Reynaud P, et al. Unsupervised and supervised classification of AE data collected during fatigue test on CMC at high temperature. *Composites Part A-Applied Science & Manufacturing*, Vol. 43, No. 2, pp 254-260, 2012.

[14]M. Johnson. Waveform based clustering and classification of AE transients in composite laminates using principal component analysis. *NDT&E International*, Vol. 35, No.6, pp 367-376, 2002.

[15]Abdi, Hervé, and Lynne J. Williams, Principal Component Analysis, Wiley Interdisciplinary Reviews: Computational Statistics, Vol. 2, No. 4, pp. 433–459, 2010.

[16]J.C. Dunn, A fuzzy relative of the ISODATA process and its use in detecting compact well-separated clusters, *Journal of Cybernetics,* Vol. 3, No. 3, pp 32–57, 1973.

[17]J. C. Bezdek. *Pattern recognition with fuzzy objective function algorithms*. 1st edition, Plenum Press, 1981.

[18]Caliński T, J H. A dendrite method for cluster analysis. *Communications in Statistics Theory and Methods*, Vol. 3, No. 1, pp 1-27, 1974.

[19]Davies DL, Bouldin DW. A Cluster Separation Measure. *IEEE Transactions on Pattern Analysis and Machine Intelligence*, Vol. 1, No. 2, pp 224-227, 1979.

[20]Rousseeuw P. Silhouettes: a graphical aid to the interpretation and validation of cluster analysis. *Journal of Computational and Applied Mathematics*, Vol. 20, No. 1, pp 53-65, 1987.